Optomechanical Variations in Cold-Drawn Thermally Treated Polypropylene Fibers

I. M. Fouda, F. M. El-Sharkawy

Department of Physics, Faculty of Science, University of Mansoura, Mansoura, Egypt

Received 12 August 2002; accepted 31 December 2002

ABSTRACT: A two-beam polarizing interference microscope with a microstrain device was used for measuring some optical and mechanical parameters for polypropylene (PP) fibers at room temperature (28 ± 1°C). The changes in the molecular orientation were evaluated to obtain orientation factors $f_2(\theta)$, $f_4(\theta)$, $f_6(\theta)$, $\langle P_2(\cos\ \theta)\rangle$, $\langle P_4(\cos\ \theta)\rangle$, and crystalline and amorphous orientation functions F_c and F_a, respectively. The shrinkage factor, uniaxial tension, true stress, molar refractivity R, surface reflectivity R', the crosslink density N_s, the chain entanglement density N_c, the segment anisotropy γ_s, and the number of chains N' were calculated. In addition, the shrinkage stress was found to increase with the increase of draw ratio. The dielectric constant ε, the dielectric susceptibility η, the average work per chain w', and the constants of the stress–birefringence equation were obtained. Comparison between Hermans's optical orientation functions and the corrected formulas by de Vries are given. The values of fully oriented refractive indices n_1 and n_2 were found. The generalized Lorentz–Lorenz equation given by de Vries was used to determine the structural parameters of PP fibers. An empirical formula was suggested to correlate the changes in the evaluated parameters with different draw ratios, and its constants were determined. The study demonstrated changes on the molecular orientation factors and evaluated microstructural parameters as a result of an applied cold-drawing process. Relationships between the calculated parameters and the draw ratios, together with microinterferograms were presented for illustration. © 2003 Wiley Periodicals, Inc. J Appl Polym Sci 90: 729–738, 2003

Key words: polypropylene fibers; optics; orientation; dielectric properties; refractive index

INTRODUCTION

Recently the interferometric methods applied to fibrous materials have been discussed extensively by many authors. For optically anisotropic fibers the refractive index and the double refraction are parameters that characterize the structure of the material. The double refraction of fibers arises from the orientation of the polymer molecules along the fiber axis, averaged over the crystalline and noncrystalline regions of the fibers. This molecular orientation influences not only the mechanical properties, but also other physical properties of the yarn.

Besides the various techniques (i.e., IR, UV, NMR, and ESR) refractive index and birefringence measurements still constitute a valuable method for the characterization of fibers. The refractive indices of fibers indicate the molecular packing density of the fibers along the directions measured. The difference between the refractive index along the axial ($n^{\parallel}$) and the radial ($n^{\perp}$) direction of fibers [i.e., birefringence (Δn)] gives the overall degree of molecular orientation of the fiber. Because most thermoplastic polymers are semicrystalline, Δn represents the overall chain orientation in the crystalline domain and is expected to have positive birefringence because of the better alignment and orientation of molecules along the fiber axis in both the crystalline and noncrystalline domains.[1–3]

Birefringence is a measure of the total molecular orientation of a system and is an excellent property to use for the study of orientation in polycrystalline polymers. Given that birefringence is a measure of the total molecular orientation of the phases present in the system, its examination in conjunction with other physical measurements (e.g., crystallinity, density, viscoelastic properties) yields considerable insight into the characteristics of the bulk polymer. The changes in optical anisotropy and orientation in polymer fibers can be evaluated interferometrically by the measurement of their refractive indices and birefringence. These optical properties provide characterization for the structure of the polymer at the molecular level. Annealing of fibers can be tested by measurement of optical anisotropy. Double-beam and multiple-beam interferometry have been used to measure refractive indices and birefringence of fibers.[4]

The most readily available techniques for changing the physical properties of polymeric structures are thermal and mechanical processes.[5–7] Mechanical treatments are used to vary the degree of orientation and other physical properties in polymeric materials.

Correspondence to: I. Fouda (ifouda@yahoo.com).

Journal of Applied Polymer Science, Vol. 90, 729–738 (2003)

To elucidate the structural variations induced in fibers by any physical and chemical modifications, the use of interferometric and acoustic methods are very useful tools. The orientation factors of fibers are well established, and often evaluated from the optical birefringence[8–10] or sonic modules.[11,12] In this study the optical parameters for thermally treated polypropylene fibers having different stress–strain conditions are used to calculate some structural parameters. Relationships are given between the obtained structural parameters.

THEORETICAL CONSIDERATIONS

The two-beam interference technique[13] was used to determine the refractive indices along and across the fiber, respectively. Also the acoustic technique was used to measure the density parameter. Obtained values were used to calculate the number of molecules per unit volume, virtual refractive index, stress optical coefficient, configuration parameter, and other structural parameters by application of suitable equations given elsewhere.[14,15]

Hermans's orientation functions

Hermans represented the orientation function $f(\theta)$ by a series of spherical harmonics (Fourier series) as follows[16]:

$$f(\theta) = \sum_{m=0}^{\infty} (m + \tfrac{1}{2})\langle f_m \rangle f_m(\theta) \tag{1}$$

where the odd components are all zero and the first three even components are given by $f_2(\theta)$, $f_4(\theta)$, and $f_6(\theta)$. The parameters $\langle f_m \rangle$ are the average values (amplitudes). A sample with orientation function may be considered to consist of perfectly aligned molecules of the mass fraction f and randomly oriented molecules of the mass fraction $(1 - f)$. f is proportional to the birefringence (Δn) as follows:

$$f_2 = \frac{\Delta n}{\Delta n_{\max}} \tag{2}$$

where $\Delta n_{\max}$ is the maximum birefringence.

Molecular orientation

On the aggregate model the low strain mechanical anisotropy is related to the orientation functions $\langle P_2(\cos\theta)\rangle$ and $\langle P_4(\cos\theta)\rangle$. These functions provide some understanding of the mechanism of deformation. By considering the network as freely oriented chains of identical links called random links[17,18] and using the Treloar[19] expression for the inverse Langevin function, we can get $\langle P_2(\cos\theta)\rangle$ and $\langle P_4(\cos\theta)\rangle$.

Isotropic refractive index[20]

Because most macromolecular crystals are birefringent, an appropriate average refractive index must be used and can be given by the following equation:

$$\bar{n}_{\text{iso}} = (n_{\perp}^2 n_{\parallel})^{1/3} \tag{3}$$

De Vries[21] defined the invariant refractive index, which he called the "virtual refractive index" n_v,[22] which replaces $\bar{n}$, the mean refractive index.

The contributions by Hermans and Platzek[23] and Kratky[24] can be given by the following equation:

$$(1 + a) = \frac{2n_1^2 n_2^2}{n_v^3(n_1 + n_2)} \tag{4}$$

From eq (4), the constant a was calculated and found to be 0.5.

Average optical orientation[25]

The overall orientation F_{av} was calculated from birefringence measurements on individual fibers. The average orientation F_{av} was calculated from the following equation:

$$F_{\text{av}(2)} = \left[\frac{2\Delta n}{\Delta n_c^{\circ} + \Delta n_a^{\circ}}\right] \tag{5}$$

where the denominator is composed of the intrinsic birefringence of crystals and the ideal amorphous birefringence, and the values used were $\Delta n_c^{\circ} = 0.0291$, $\Delta n_a^{\circ} = 0.060$, and $\Delta n_{\max}^{\circ} = 0.045$.[25]

The intrinsic birefringence values are not constant because of variations in the structure configuration[12] of PP fibers.

Shrinkage stress

The shrinkage on fibers is related to the extension ratio D (final fiber length/starting length) by the following relation[26]:

$$S = (D - 1)D \tag{6}$$

This gives $D = 1/(1 - S)$, which explains the use of the factor $[1/(1 - S)^2 - (1 - S)]$ as the ordinate in this figure. If the shrinkage force could be measured, the stress optical coefficient can be used to calculate the number of monomer unit per link.

Calculation of dielectric constant and magnetic susceptibility

The dielectric constant $\varepsilon_\perp$, measured radially, is different from that of $\varepsilon_\parallel$, measured axially; the fiber has two different dielectric constants; it is anisotropic with respect to its dielectric[22]:

$$\varepsilon = \frac{1 + 2(\bar{n}^2 - 1/\bar{n}^2 + 2)}{1 - (\bar{n}^2 - 1/\bar{n}^2 + 2)} \tag{7}$$

where $\bar{n}$ is the refractive index, and $n_\parallel$ and $n_\perp$ are the refractive indices radially and axially, respectively. There are analogous equations for $\varepsilon_\parallel$ and $\varepsilon_\perp$. The dielectric constant varies according to the way in which the fiber is arranged (i.e., to the degree of orientation).

The dielectric susceptibility η is related to ε and analogous equations for $\eta_\parallel$, $\eta_\perp$, and η were given.[27]

Molar refractivity[28]

The polarizability of a molecule is related to its refractive index by the Lorentz–Lorenz relation:

$$\frac{\bar{n}^2 - 1}{\bar{n}^2 + 2}\left(\frac{M}{\rho}\right) = R \tag{8}$$

where ρ is the density, M is the molecular weight, and R is the molecular or molar refractivity. The value M used is that of the repeat unit of the molecule; the density used for bulk PP = 0.869 gm/cm^3. In the present work we considered the density of PP constant for different draw ratios because of the great difficulties in evaluation.

The surface reflectivity

The surface reflectivity of polymer for light at normal incidence can be estimated from Fresnel's equation[29] and the mean refractive index $\bar{n}$. Thus the percentage reflection R' (in air) is given by

$$R' = \left(\frac{\bar{n} - 1}{\bar{n} + 2}\right)^2 \times 100 \tag{9}$$

The average work per chain for a collection of chains will depend on the distribution of chain-end distances, and is obtained by the following equation[30]:

$$w' = \frac{3KT}{2}\left[\tfrac{1}{3}(D^2 - D^{-1}) + (D^{-1} - 1)\right] \tag{10}$$

Also the theory for the stress–optical behavior of rubbers was first developed by Kuhn and Grun[42] for uniaxial deformation. The tensile stress σ produced by the uniaxial extension of rubber network to an extension ratio D is given by

$$\sigma = NKT[D^2 - D^{-1}] \tag{11}$$

where K is Boltzmann's constant, T is the absolute temperature, and N is the number of network chains per unit volume.

Moony–Rivlin constants

To fit the Ball model[30] to the experimental data, initial estimates of the model parameters are needed. These were obtained using Moony–Rivlin plots where the reduced stress σ^* is expressed as

$$\sigma^* = \frac{\sigma}{[D_{\max}^2 - D_{\min}^2]} \tag{12}$$

$$\sigma^* = [C_1 + C_2 D^{-1}] \tag{13}$$

where C_1 and C_2 are empirical constants called the Moony–Rivlin coefficients, which can be related approximately to the structure of the network parameters N_s, the crosslink density, and N_c, the chain entanglement density, where

$$N_s = C_1/KT \quad \text{and} \quad N_c = C_2/KT$$

The estimate of N_c, however, is not strictly correct because C_2 also relates to the link effectiveness. Because the Moony–Rivlin plots obtained from the deformation of polypropylene fiber are not linear over the whole strain range, the data points on the initial linear part of the curve were used to give values of $N_s = 6.4066 \times 10^{27}$ and $N_c = 1.516 \times 10^{26}$.

Evaluation of the stress optical coefficient and segment anisotropy[31]

When the contributions of the chains to the network anisotropy are summed, and the Lorentz–Lorenz relation used to obtain the birefringence between the refractive index parallel $n^\parallel$ and perpendicular $n^\perp$ to the extension directions, the result is[32]

$$n^\parallel - n^\perp = \frac{N'\gamma_s}{90\Psi}\frac{[\bar{n}^2 + 2]^2}{\bar{n}}[D^2 - D^{-1}] \tag{14}$$

where N' is the number of chains between crosslinks per unit volume at absolute temperature and Ψ is the permittivity of free space [8.85 $\times$ 10^{-12} fm^{-1} (m^{-3} kg^{-1} S^4 A^2)].

$$C_s = \frac{\gamma_s}{90\Psi KT}\frac{[\bar{n}^2 + 2]^2}{\bar{n}} \tag{15}$$

where C_s is the stress optical coefficient and γ_s is the segment anisotropy. From eqs (14) and (15) we can determine γ_s and then N'.

The birefringence of partially crystalline polymers

Assuming that partially crystalline polymers consist of separate crystalline and amorphous phases, the change in crystal direction on stretching was affine with the deformation of the amorphous matrix, but the crystal did not change in size on stretching.

If there are Y crystals per unit volume, and these have polarizabilities α_c along the c-axis and $\alpha_b = \alpha_a$ perpendicular to it, then the crystal contribution to the birefringence of the medium is given by[32,33]

$$[n^{\parallel} - n^{\perp}] = \frac{[\bar{n}^2 + 2]}{\bar{n}} \frac{Y}{18\Psi_0} [\alpha^{\parallel} - \alpha^{\perp}] \langle P_2(\cos^2\theta_c) \rangle \qquad (16)$$

where $P_2(\cos^2\theta_c)$ is the orientation of the stretching function.

Degree of crystallinity

The crystallinity in weight fraction (χ_w) was obtained with the following relation:

$$\chi_w = \frac{\rho_c(\rho - \rho_a)}{\rho(\rho_c - \rho_a)} \times 100 \qquad (17)$$

where ρ_c and ρ_a are the densities of the crystallinity and amorphous phases, respectively. In this estimation values of 0.946 and 0.854 g/cm^3 were assumed for ρ_c and ρ_a, respectively.[34]

Amorphous orientation

The amorphous orientation function F_a was calculated by the following equation[35]:

$$\Delta n = \Delta n_{c_0} F_c \chi_w + \Delta n_{a_0} F_a (1 - \chi_w) \qquad (18)$$

where χ_w is the degree of crystallinity; Δn_{c_0} and Δn_{a_0} are the intrinsic birefringence of the crystalline and noncrystalline regions, respectively; and $F_c = (D^3 - 1)/(D^3 + 2)$.[36]

EXPERIMENTAL

Preparation of samples by annealing process

The polypropylene (PP) fibers were wound in a cocoon form on a glass rod with free ends, after which they were annealed in an electric oven. The temperature was adjusted to 70, 100, and 130 ± 1°C with constant annealing times of 4 h, and then left to cool in air at 28 ± 1°C.

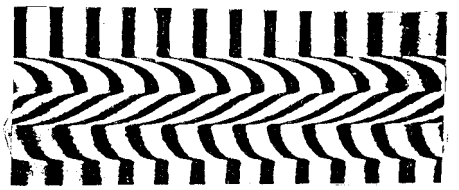

Plate (1-a)

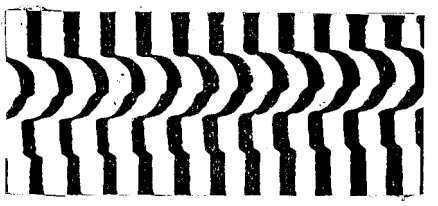

Plate (1-b)

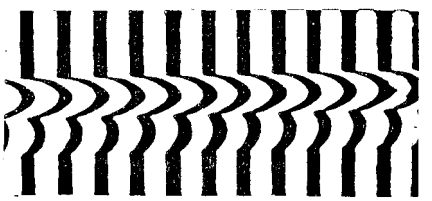

Plate (1-c)

Plate 1 Interferograms from the totally duplicated image position for different draw ratios at constant annealing temperature (100 ± 1°C).

Application of two-beam interferometry

Fibers with different draw ratios were examined by the double refracting interference Pluta microscope (Poland). Plate 1(a)–(c) is an example of the obtained interferograms of two-beam interferometry from the totally duplicated image position for different draw ratios at a constant annealing temperature 100 ± 1°C. The plane polarized light of λ = 546 nm, vibrating along and across the fiber axis, and the refractive index of the immersion liquid were selected to allow the fringe shift to be small. The corresponding results of draw ratios and optical parameters are given in Table I.

Evaluation of optical and structural parameters such as isotropic refractive index (n_{iso}) and virtual

TABLE I
Values of Draw Ratio, Isotropic Refractive Index, Virtual Refractive Index, Dielectric Constant, and Dielectric Susceptibility, Along and Across the Fiber Axis

Draw ratio	n_{iso}	n_v	$\varepsilon^{\parallel}$	$\varepsilon^{\perp}$	$\bar{\varepsilon}$	$\eta^{\parallel}$	$\eta^{\perp}$	$\bar{\eta}$
A. For unannealed PP fiber								
1	1.500	1.500	2.256	2.247	2.250	0.0999	0.0992	0.0994
3	1.510	1.510	2.326	2.259	2.281	0.1055	0.1002	0.1019
5	1.511	1.511	2.332	2.259	2.283	0.1059	0.1002	0.1021
6	1.512	1.511	2.338	2.259	2.285	0.1064	0.1002	0.1022
B. For PP fiber at constant temperature 70°C								
1	1.501	1.501	2.268	2.247	2.254	0.1009	0.0992	0.0998
3	1.494	1.494	2.277	2.211	2.233	0.1016	0.0963	0.0981
5	1.495	1.495	2.283	2.211	2.235	0.1021	0.0963	0.0982
6	1.495	1.495	2.286	2.211	2.236	0.1023	0.0963	0.0983
C. For PP fiber at constant temperature 100°C								
1	1.491	1.491	2.208	2.229	2.222	0.0961	0.0978	0.0972
3	1.497	1.497	2.280	2.223	2.242	0.1018	0.0973	0.0988
5	1.498	1.498	2.286	2.223	2.244	0.1023	0.0973	0.0990
7	1.498	1.497	2.289	2.220	2.243	0.1026	0.0971	0.0989
D. For PP fiber at constant temperature 130°C								
1	1.493	1.493	2.202	2.244	2.230	0.0956	0.0990	0.098
2	1.505	1.505	2.292	2.253	2.266	0.1028	0.0997	0.101
3	1.506	1.506	2.295	2.253	2.267	0.1030	0.0997	0.101

refractive index (n_v) were calculated. The resultant data of these parameters are given in Table I. The relationship between Δn and differences in the isotropic and virtual refractive indices ($n^{\parallel} - n_v$, $n^{\perp} - n_v$, $n^{\parallel} - n_{iso}$, and $n^{\perp} - n_{iso}$) are given in Figure 1. The values of virtual refractive index and maximum birefringence were used in Figure 1 to predict the values of the values of the refractive indices n_1 and n_2 for fully oriented PP fibers. Values of n_1 and n_2 were found to be 1.552 and 1.507, respectively, at 28 ± 1°C, in agreement with previously published values.

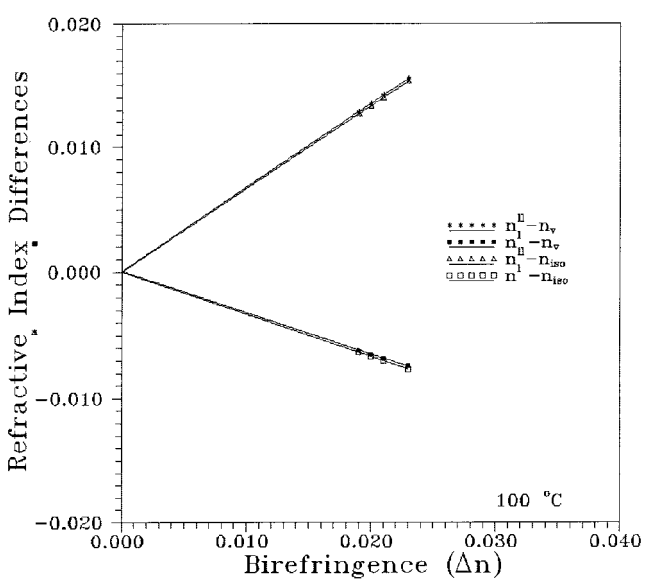

Figure 1 Relationship between the birefringence Δn and the refractive indices differences ($n^{\parallel} - n_v$, $n^{\perp} - n_v$, $n^{\parallel} - n_{iso}$, and $n^{\perp} - n_{iso}$) of PP fiber at different draw ratios and different annealing temperature (at 100°C).

In view of the relevance of the optical orientation functions given by Hermans, $f_2(\theta)$, $f_4(\theta)$, and $f_6(\theta)$, to the deformation mechanism, it is interesting to calculate their values, presented in Figure 2 with different draw ratios and at different annealing conditions.

Figure 3 shows the relationship between the optical orientation [$P_2(\theta)$ and $P_4(\theta)$] and draw ratio at constant annealing temperature for PP fibers.

The dielectric constant ε and the dielectric susceptibility η were determined from eq (7) to obtain dielectric susceptibility. The resultant data for $\varepsilon^{\parallel}$, $\varepsilon^{\perp}$, ε, $\eta^{\parallel}$, $\eta^{\perp}$, and η are given in Table I, where $\varepsilon^{\parallel}$ and $\eta^{\parallel}$ are increased as a result of the increase of draw ratios and $\varepsilon^{\perp}$ and $\eta^{\perp}$ are decreased.

Figure 4 shows the relationship between the average optical orientation function F_{av} and draw ratio at constant annealing temperature for PP fibers. F_{av} increases with different draw ratios as the temperature of annealing increases.

Figure 5 shows the relationship between draw ratio and the shrinkage stress S for PP fibers at different annealing temperatures. S increases with different draw ratios as the temperature increases.

The surface reflectivity R' was estimated from eq (9) and is shown in Figure 6, where surface reflectivity increases as the draw ratio increases at different annealing temperatures for PP fibers.

Figure 7 shows the variation between the tensile stress σ and draw ratio at different annealing temperatures for PP fibers. The value of σ increases with different draw ratios as the temperature increases.

Figure 8 shows the relationship between draw ratio and the stress optical coefficient C_s for PP fibers at different annealing temperatures.

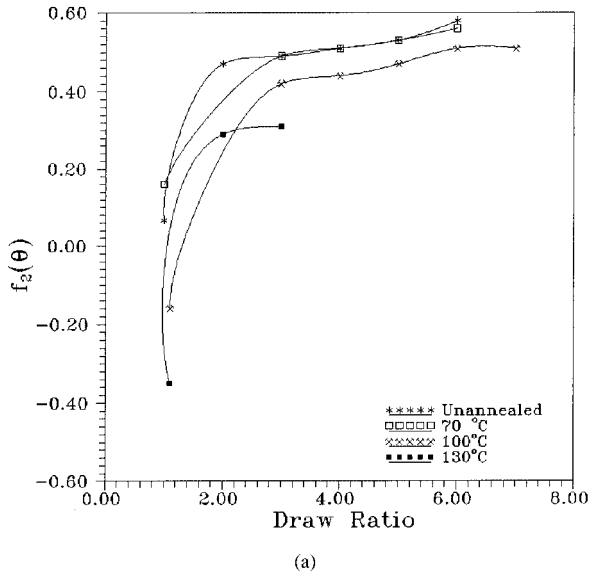

(a)

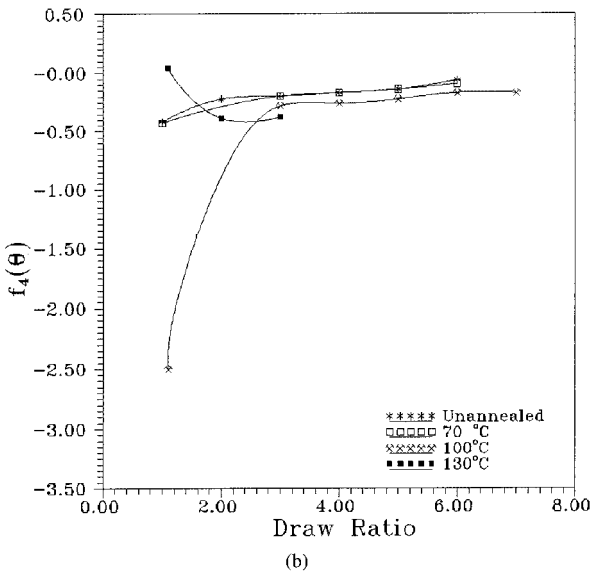

(b)

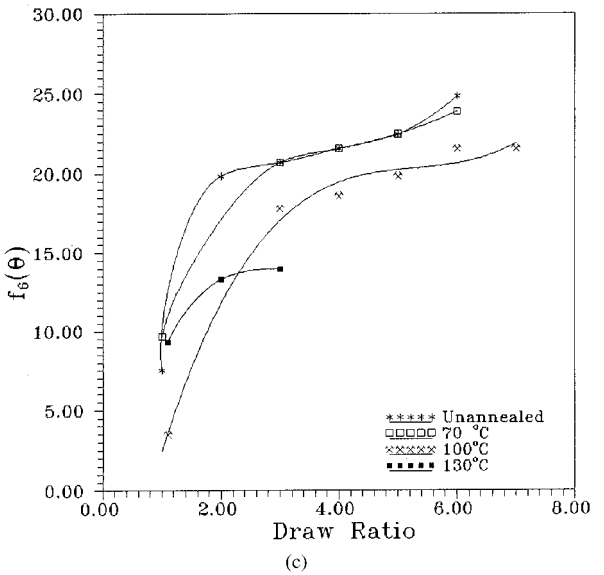

(c)

Figure 2 Relationship between the optical orientation functions $f_2(\theta)$, $f_4(\theta)$, and $f_6(\theta)$ and draw ratio at different temperatures for PP fibers.

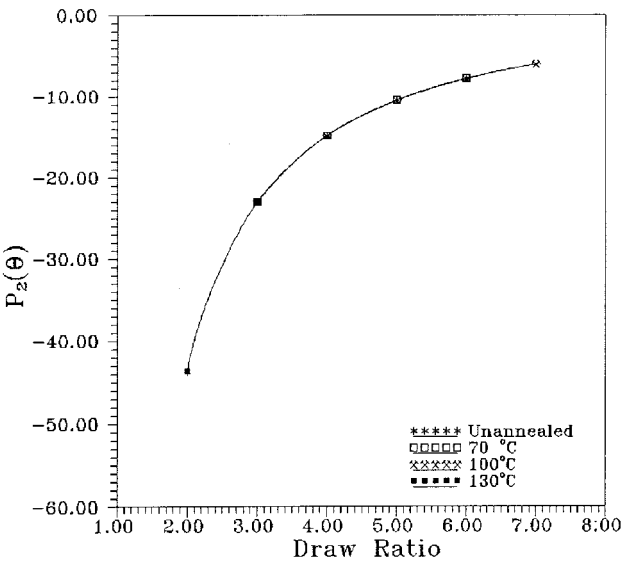

(a)

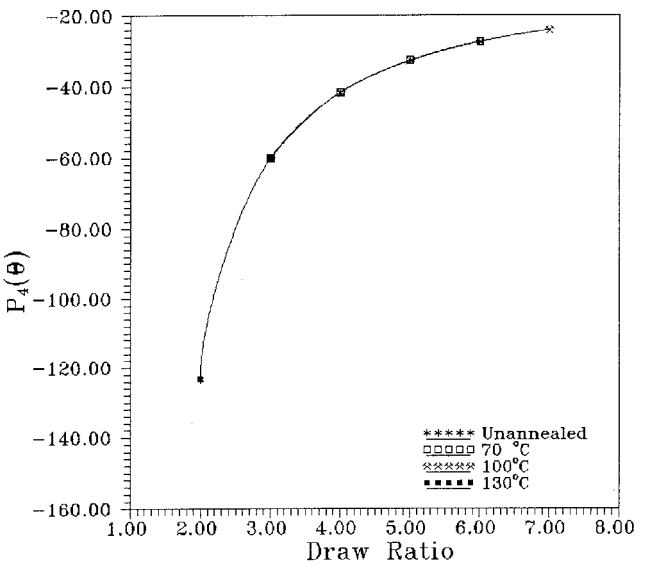

(b)

Figure 3 Relationship between the optical orientation functions $P_2(\theta)$ and $P_4(\theta)$ and draw ratio at different temperatures for PP fibers.

Figure 9 shows the relationship between draw ratio and the segment anisotropy γ_s for PP fibers at different annealing temperatures.

In Table II the average work per chain w', the average orientation angle on uniaxial stretching $\langle \cos^2\theta_c \rangle$, the amorphous orientation function F_a, the crystalline orientation function F_c, the number of network chains per unit volume N, and the number of chains N', with

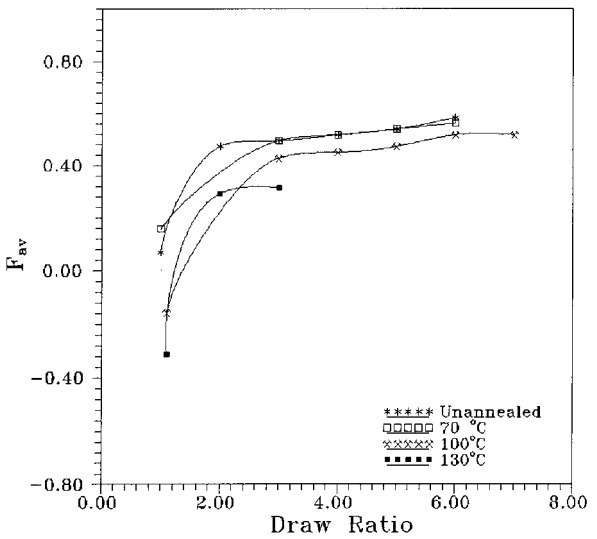

Figure 4 Average orientation F_{av} and draw ratio at different temperatures for PP fibers.

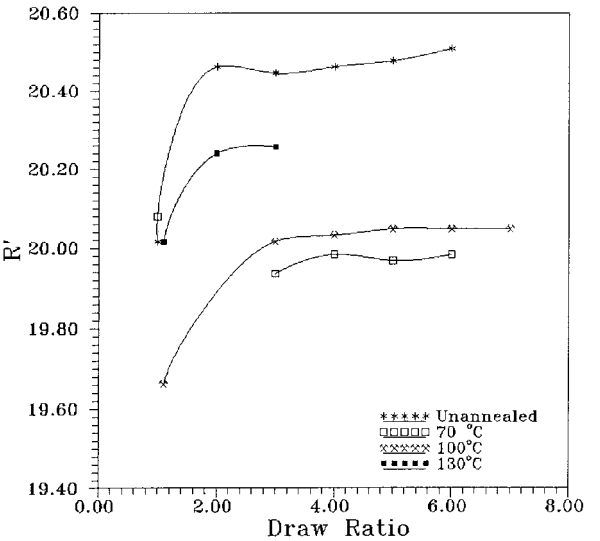

Figure 6 Relationship between the surface reflectivity R' and draw ratio at different annealing temperatures for PP fibers.

different draw ratios at different annealing conditions for PP fibers, are given. The values of molar refractivity R are also given in Table II, where the molar reflectivity increases as the draw ratio and annealing temperature increase.

Figure 10 shows the relationship between draw ratio and the crystal per unit volume Y at different annealing temperatures for PP fibers. The value of Y decreases with different draw ratios as the temperature increases.

Figure 11 shows the relationship between crystallinity χ and annealing temperature for PP fibers. The value of χ increases as the annealing temperature increases.

RESULTS AND DISCUSSION

Drawing of macromolecular samples represents one of the most extensive changes in orientation of the polymer chains. In most instances the chain orients parallel to the draw direction. Our present results make clear that new orientations occur as a result of cold drawing at various draw ratios. The degree of orientation and other structural parameters, such as ω', F_c, F_a, and χ, for instance, are correlated to the end use of the final fiber.

The effects of orientation on the physical properties of polymers are profound, generally in the expected direction of increased tensile strength and stiffness with increasing orientation. As orientation is in-

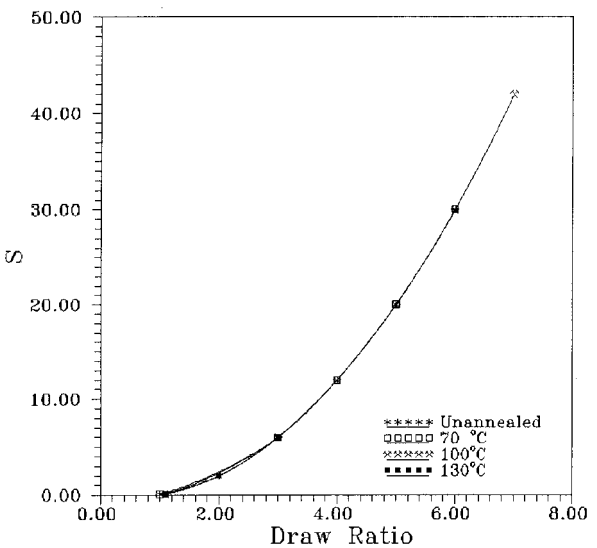

Figure 5 Relationship between draw ratio and the shrinkage stress S for PP fibers at different annealing temperatures.

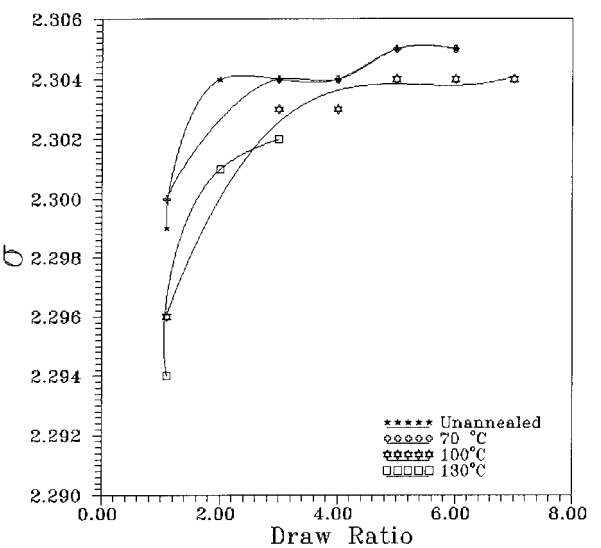

Figure 7 Relationship between the tensile stress σ and draw ratio at different annealing temperatures for PP fibers.

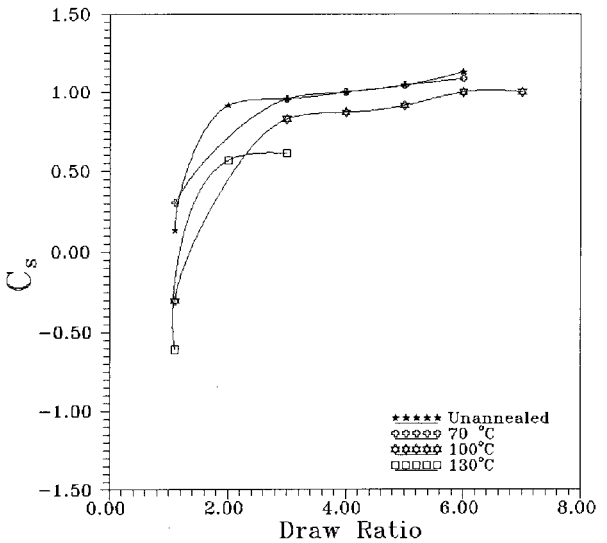

Figure 8 The stress optical coefficient C_s against draw ratio at different temperatures for PP fibers.

creased, anisotropy of the mechanical properties becomes evident. At the same time the physical properties of the sample change significantly.[37]

Thermomechanical history, such as annealing influences, the ability of materials to undergo plastic deformation, and annealing effects on polypropylene fibers, have been previously reported.[12,38–40] Annealing renders a polymer stiffer and more brittle. At the microstructural level, an irreversible reorganization occurs, often leading to shrinkage, as illustrated in Figure 5.

Shrinkage stress is generated through an entropic retraction. When the internal energy of an oriented polymer is elevated by an increase in ambient temperature, polymer molecules tend to relax the orientation by retracting from an ordered, extended conformation to a disordered, random coil. This eventually produces a change of length or contraction force.[37] Shrinkage stress can be observed through the measurement of the force exerted on the constraints with fixed ends, as calculated from the mean refractive index.

Under a given external force, different materials will exhibit different types of deformation response. In the mechanical vein, elastomers must stretch rapidly under tension with little loss of energy as heat, which could be felt as a result of the change in entropy. When stress is released, they recover their original dimensions with rebound. Therefore the recovery achieved is indicated by shrinkage parameters. Finally, there is the importance of molecular orientations in determining physical properties, especially mechanical properties. The deformation scheme that describes the results obtained assumes that the polymer consists of an aggregate of transversely isotropic units whose symmetry axes rotate on drawing in the same manner as lines joining pairs of points in the bulk material, which deforms at constant volume. Hence the mechanical anisotropy for crystalline polymer and glassy polymer, deformed by cold drawing, enables the factor $P_4(\theta)$ together with $P_2(\theta)$ to be calculated as a function of draw ratio.[8,26]

The change in fiber density is an indication of a change in volume attributed to the mass redistribution associated with the annealing and drawing processes. This change in volume affects some other parameters, such as N_s, N_c, C_s, γ_s, ε, η, F_c, and F_a. This may be because of changes of the free volume area spaces, which can be represented by mobile voids moving freely about in the structure by stretching. An alternative view is that the change in obtained optical birefringence results from the polymer material having two or more separate phases with different refractive indices. The birefringence of a crystalline polymer is made up of contributions from the crystalline and amorphous regions plus an additional contribution from birefringence, resulting from the shape of the crystal or the presence of voids.

CONCLUSIONS

From the calculations carried out in the present work and the changes in the optical structural parameters attributed to the different annealing processes for polypropylene fibers, the following conclusions may be drawn:

1. Optical and mechanical orientations are different techniques that are suitable for predicting molecular orientation in PP fibers. Every technique has its own contribution, and both increase as the draw ratio increases. The two-beam interference

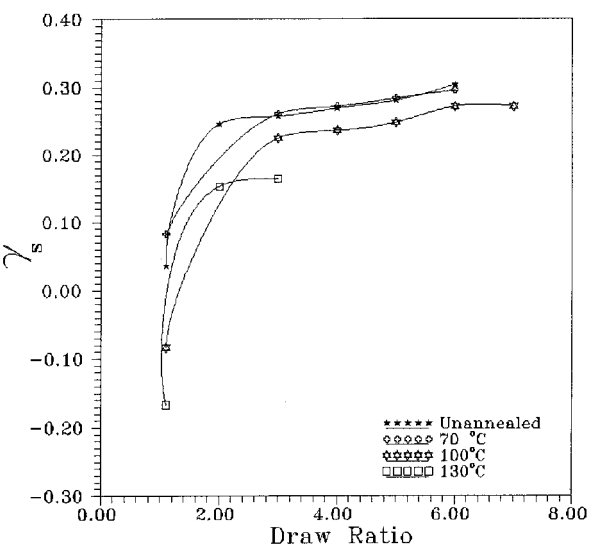

Figure 9 The segment anisotropy γ_s and draw ratio at different temperatures for PP fibers.

TABLE II
Values of Draw Ratio, Molar Refractivity, Average Work per Chain, Average Orientation Angle, Amorphous Orientation Function, Crystalline Orientation Function, Number of Network Chains per Unit Volume, and Number of Chains

Draw ratio	R	$\omega' \times 10^{-20}$	$\langle\cos^2\theta_c\rangle$	F_a	F_c	N	$N' \times 10^{18}$
A. For unannealed PP fiber							
1	14.242	—	—	—	—	—	—
3	14.490	1.396	−15.03	0.439	0.897	0.0657	0.647
5	14.506	4.691	−6.675	0.478	0.976	0.0230	0.226
6	14.521	6.981	−4.895	0.481	0.986	0.0159	0.157
B. For PP fiber at constant temperature 70°C							
1	14.274	—	—	—	—	—	—
3	14.104	1.396	−15.03	0.437	0.897	0.0657	0.647
5	14.120	4.691	−6.675	0.476	0.976	0.0230	0.226
6	14.128	6.981	−4.895	0.480	0.986	0.0159	0.156
C. For PP fiber at constant temperature 100°C							
1	14.016	—	—	—	—	—	—
3	14.177	1.396	−15.03	0.437	0.897	0.0657	0.647
5	14.193	4.691	−6.675	0.476	0.976	0.0230	0.226
7	14.185	9.693	−3.701	0.483	0.991	0.0117	0.115
D. For PP fiber at constant temperature 130°C							
1	14.081	—	—	—	—	—	—
2	14.370	0.419	−28.79	0.341	0.700	0.163	1.60
3	14.378	1.396	−15.03	0.438	0.897	0.066	0.65

with a microstrain device is suitable for determining many structural parameters with fair accuracy.

2. The shrinkage stress is related to the draw ratio and is also related to the orientation, optical parameters, and number of crystals, for instance.
3. As the draw ratio increases, the double refraction increases. Furthermore this means an increase in the inherent optical anisotropy of the chainlike macromolecules from the preferred axial orientation of the molecular chains that constitute the fiber.
4. As the draw ratio increases, the orientation factors increase. The higher the orientation factor, the more mutually parallel the molecules and the smaller the average angle formed by them within the fiber axis. Also the amorphous regions decrease, which is of practical importance for studying the nature of swelling and diffusion of dyes, although this would be the subject of further studies.
5. The parameter $P_4(\theta)$ is always comparatively small; thus the mechanical method could be used

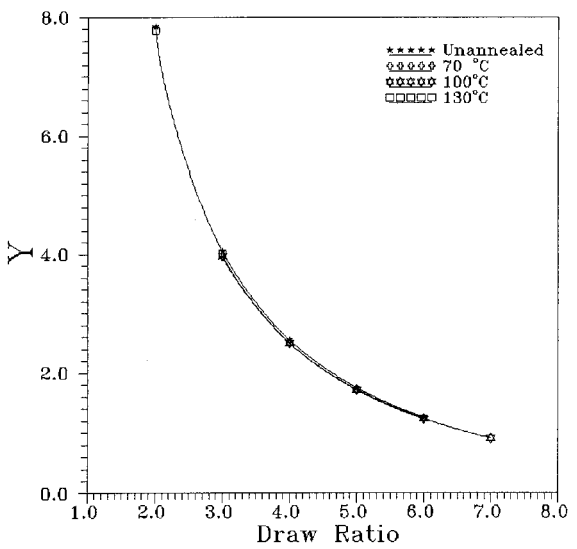

Figure 10 Relationship between draw ratio and the crystal per unit volume Y at different annealing temperatures for PP fibers.

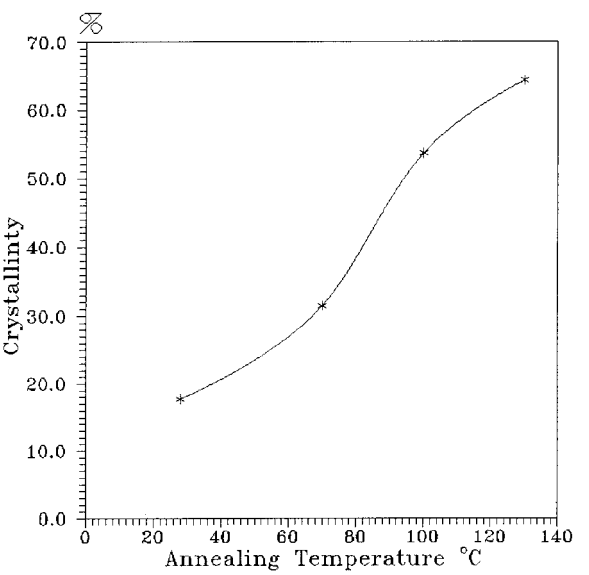

Figure 11 Relationship between crystallinity χ_w and annealing temperature for PP fibers.

for determining the orientation parameters $P_2(\theta)$ and $P_4(\theta)$.

6. The obtained principal optical parameters are suitable for evaluating the dielectric constant, the dielectric susceptibility, and surface reflectivity in fibers. Also the average work per chain (w') increases with increasing draw ratios.
7. Comparison between the obtained values of isotropic and virtual refractive indices shows that the values of n_{iso} and n_v are nearly the same, although each equation has its own merit.

From the above results and considerations, we conclude that the thermal treatments and drawing are sensitive to variations in the optical structural parameters and other physical properties in polymeric materials.

References

1. Timm, D. A.; You-Lottsieh J Polym Sci Part B: Polym Phys 1993, 31, 1873.
2. Barakat, N.; Hamza, A. A. Interferometry of Fibrous Materials; Hilger: Bristol, UK, 1990.
3. Fouda, I. M.; Seisa, E. A.; Oraby, A. H. J Appl Polym Sci 1999, 71, 361.
4. Nobbs, J. H.; Bower, D. I.; Ward, I. M.; Patterson, D. Polymer 1974, 15, 28.
5. William, G.; Perkins, P.; Porter, S. R. J Mater Sci 1977, 2355.
6. Statton, W. O. J Polym Sci Polym Phys Ed 1975, 13, 835.
7. Fouda, I. M.; Shabana, H. J Appl Polym Sci 1999, 72, 1185.
8. Ward, I. M. Mechanical Properties of Solid Polymers, 2nd ed.; Wiley: New York, 1983.
9. Ward, I. M. Structure and Properties of Oriented Polymers; Elsevier Applied Science: London, 1975.
10. Cunningham, A.; Ward, I. M.; Willis, H. A.; Zichy, V. Polymer 1974, 15, 749.
11. Dumbleton, J. H. J Polym Sci Part A-2 1968, 6, 795.
12. Samules, R. J. Structural Polymer Properties; Wiley: New York, 1974; p. 50.
13. Barakat, N.; Hamza, A. A. Structural Polymer Properties; Wiley: New York, 1974; p. 2.
14. Fouda, I. M.; Shabana, H. M. Polym Compos 1999, 7, 333.
15. Hamza, A. A.; Fouda, I. M.; Kabeel, M. A.; Shabana, H. M. Polym Test 1996, 15, 301.
16. Gedde, U. F. W. Polymer Physics; Chapman & Hall: London, 1995; p. 214.
17. Stein, R. S. J Polym Sci 1959, 24, 709.
18. Hermans, P. H. Contributions to the Physics of Cellulose Fibers; North-Holland: Amsterdam, 1946; Chapters 3 and 4.
19. Treloar, L. R. G. The Physics of Rubber Elasticity, 2nd ed.; Oxford University Press: London, 1958.
20. Zbinden, R. Infrared Spectroscopy of High Polymers; Academic Press: New York, 1964.
21. de Vries, H. Kolloid Z Z Polym 1979, 257, 226.
22. Moncrieff, R. W. Man-Made Fibers, 6th ed.; Newnes Butterworths: London, 1975.
23. Hermans, P. H.; Platzek, P. Z Kolloid 1939, 88, 67.
24. Kratky, O. Z Kolloid 1933, 64, 213.
25. Wesolowska, E.; Lewaskiewicz, W. J Polym Sci Polym Phys Ed 1988, 26, 2573; cited in Murthy, N. S.; Bray, R. G.; Carreale, S. T.; Moore, R. A. F. Polymer 1995, 36, 3863.
26. Ward, I. M. J Polym Sci Polym Symp 1977, 58, 1.
27. Born, M.; Wolf, E. Principles of Optics, 2nd ed.; Pergamon Press: London, 1964; p. 88.
28. Hemsley, D. A. Applied Polymer Light Microscopy; Elsevier Press: London, 1989; pp. 7, 193.
29. Williams, D. J. Polymer Science and Engineering; Prentice Hall: London, 1971; p. 190.
30. Ball, R. C.; Doi, M.; Edward, S. F.; Warner, M. Polymer 1981, 22, 1010; cited in Mattews, R. G.; Duckett, R. A.; Ward, I. M. Polymer 1997, 38, 4795.
31. Riande, E.; Guzman, J. J Polym Sci Polym Phys Ed 1984, 22, 917.
32. Jenkins, A. D. Materials Science Handbook: Polymer Science; North-Holland: Amsterdam, 1972; Vol. 1, Chapter 7.
33. Hamza, A. A.; Fouda, I. M.; Sokkar, T. Z.; Shahin, M. M.; Seisa, E. A. J Mater Sci 1995, 30, 2597.
34. Wunderlich, B. Macromolecular Physics; Academic Press: New York, 1973; Vol. 1, p. 388.
35. Stein, R. S.; Norris, F. H. J Polym Sci 1956, 21, 381.
36. Bourvelles, G. L.; Beautemps, J. J Appl Polym Sci 1990, 39, 329.
37. Billmeyer, F. W. Textbook of Polymer Science, 3rd ed.; Wiley-Interscience: London, 1965; p. 224.
38. Trznadel, M.; Kryszewski, M. J Macromol Sci Rev Macromol Chem Phys 1992, 32, 259.
39. Yefinov, A. V.; Lapshin, V. P.; Fartunin, V. I.; Vozlov, V. P.; Bakeyev, N. F. Polym Sci USSR Vysokomol Soyed 1983, A25, 692.
40. Hamza, A. A.; Fouda, I. M.; Sokkar, T. Z. N.; El-Bakary, M. A. Polym Int 1996, 39, 129.
41. Fouda, I. M. J Appl Polym Sci 1999, 73, 819.
42. Kuhn, W.; Grün, F. Kolloidzchr 1948, 101, 248.